

# Probing the structure of *Leishmania donovani chagasi* DHFR-TS: comparative protein modeling and protein–ligand interaction studies

Lakshmi Maganti · Prabu Manoharan · Nanda Ghoshal

Received: 27 November 2009 / Accepted: 22 December 2009 / Published online: 21 February 2010  
© Springer-Verlag 2010

**Abstract** Dihydrofolate reductase (DHFR) has been used successfully as a drug target in the area of anti-bacterial, anti-cancer and anti-malarial therapy. It also acts as a drug target for Leishmaniasis. Inhibition of DHFR leads to cell death through lack of thymine (nucleotide metabolism). Although the crystal structures of *Leishmania major* and *Trypanosoma cruzi* DHFR-thymidylate synthase (TS) have been resolved, to date there is no three-dimensional (3D)-structural information on DHFR-TS of *Leishmania donovani chagasi*, which causes visceral leishmaniasis. Our aim in this study was to model the 3D structure of *L. donovani chagasi* DHFR-TS, and to investigate the structural requirements for its inhibition. In this paper we describe a highly refined homology model of *L. donovani chagasi* DHFR-TS based on available crystallographic structures by using the *Homology* module of Insight II. Structural refinement and minimization of the generated *L. donovani chagasi* DHFR-TS model employed the *Discover 3* module of Insight II and molecular dynamic simulations. The model was further validated through use of the PROCHECK, Verify\_3D, PROSA, PSQS and ERRAT programs, which confirm that the model is reliable. Superimposition of the model structure with the templates *L. major* A chain, *L. major* B chain and *T. cruzi* A chain showed root mean square deviations of 0.69 Å, 0.71 Å and 1.11 Å, respectively. Docking analysis of the *L. donovani chagasi* DHFR-TS model with methotrexate enabled us to identify specific residues, viz. Val156, Val30, Lys95, Lys75 and Arg97, within the *L. donovani chagasi* DHFR-TS binding pocket, that play an important role in ligand or substrate binding.

Docking studies clearly indicated that these five residues are important determinants for binding as they have strong hydrogen bonding interactions with the ligand.

**Keywords** Leishmanial DHFR-TS · Homology modeling · Methotrexate · Docking

## Introduction

The protozoan parasite *Leishmania* species is the causative agent of leishmaniasis. Three different clinical forms of this disease, with different immunopathologies and degrees of morbidity and mortality, have traditionally been classified: visceral leishmaniasis (VL), cutaneous leishmaniasis (CL) and mucocutaneous leishmaniasis (MCL). VL, caused by *Leishmania donovani*, *L. chagasi*, *L. donovani chagasi* and *L. infantum*, is the most lethal form of the disease. The name *Leishmania chagasi* (a member of the *Leishmania donovani* complex) is frequently used for the aetiological agent of visceral leishmaniasis [1]. CL is caused by *Leishmania major*, *L. mexicana*, *L. braziliensis* and *L. panamensis* [2] and MCL is caused by *L. amazonensis*, *L. guyanensis*, *L. panamensis* and *L. aethiopica*. The general aspects of leishmaniasis and overall control strategies have been reviewed recently [3, 4]. The parasite *Leishmania* is endemic in several parts of the world and remains a serious public health problem in numerous countries. It affects 350 million people worldwide with 1–2 million new cases in each year [5].

*Leishmania* co-infection is emerging as serious problems of new diseases [6]. Drugs that are currently used to treat these diseases are toxic, expensive and have adverse side effects [7]. Effective therapy is needed for millions of already infected persons. To identify novel drug targets, it is important to understand the essential metabolic pathways of

L. Maganti · P. Manoharan · N. Ghoshal (✉)  
Structural Biology and Bioinformatics Division,  
Indian Institute of Chemical Biology (a unit of CSIR),  
Kolkata 700032, India  
e-mail: nghoshal@iicb.res.in

the parasite. Folates are essential for a number of important biochemical reactions because they serve as cofactors in a number of one-carbon transfer reactions (e.g., biosynthesis of the nucleotide dTMP) [8]. Hence, the enzymes related to this metabolism are of interest as drug targets, and the use of antifolates should in principle provide an ideal treatment [9].

Dihydrofolate reductase (DHFR) is a ubiquitous enzyme that has wide scale application as a drug target. In several species of protozoa, the catalytic activities for the enzymes DHFR and thymidylate synthase (TS) reside on a single polypeptide chain, constituting a bifunctional DHFR-TS enzyme [10, 11]. In most other species, however, these enzymes are mono-functional, with catalytic activities on separate peptides [12]. The reason for the success of DHFR as a drug target is its pivotal role in the reduction of dihydrofolate to tetrahydrofolate—an important co-factor in the biosynthesis of thymine in nucleotide metabolism (Fig. 1). In folate metabolism, DHFR and TS enzymes acts as a useful targets and are currently used for the treatment of cancer and microbial infections [13–15]. TS catalyzes the conversion of dUMP to dTMP using the cofactor N5, N10-methylene tetrahydrofolate (THF), as both the C-donor and reductant, while DHFR maintains the THF pool by the NADPH-dependent reduction of dihydrofolate (DHF). Inhibition of either enzyme limits the supply of dTMP required for DNA synthesis, thus curtailing replication and leading to cell death.

Homology modeling is known to be an efficient method for the construction of the three-dimensional (3D) structure of proteins [16–18]. The main aim of homology modeling is to build a 3D structure of a protein (if not known) from its primary structures via comparison with other known protein structures. For homology modeling, the target protein sequence should have at least 30% sequence identity to the template. In this work, we have attempted to obtain a reliable 3D structure for *L. donovani chagasi* DHFR-TS by a homology modeling procedure based on the crystal structures of *L. major* DHFR-TS [19] and *Trypanosoma cruzi* DHFR-TS [20]. The model structure was then refined by energy minimization and molecular dynamics (MD) simulations. Docking studies were performed with methotrexate (MTX). The docked complex was used to identify the important residues and to further reveal the

ligand receptor interaction mechanism, in particular, identifying residues binding with MTX, which would be helpful in designing potent inhibitors against the target.

## Theory and methods

### Computational tools

The computational studies performed in this work used the following software packages. For homology modeling, Insight II [21] studies were performed on an SGI Fuel workstation running an IRIX 6.5 operating system. For docking studies, GOLD 3.2 [22] was run on a Pentium 4 core2 Duo workstation using a Windows XP operating system. Protein–ligand interactions were observed in pymol [23].

### Template selection

The *L. donovani chagasi* DHFR-TS protein sequence (accession No. AAM88576) with a length of 520 amino acids was obtained from NCBI (<http://www.ncbi.nlm.nih.gov/>). With the help of this sequence information, a PDB-BLAST search was performed for selection of templates based on sequence identity and similarity. The PDB-BLAST search revealed that the sequence identity of *L. donovani chagasi* DHFR-TS with homologous proteins *T. cruzi* DHFR-TS and *L. major* (coordinates of *L. major* crystallographic structure kindly supplied by D. Matthews, Agouron Pharmaceuticals, San Diego, CA) are 66% and 90%, respectively. *T. cruzi* DHFR-TS was in addition to *L. major* as a template for regions in the target protein that do not match with those of *L. major* and also to compensate for gaps.

### Sequence alignment

The first requirement in the construction of a *L. donovani chagasi* DHFR-TS model structure is sequence alignment between templates and the target protein. The sequences of the target and templates *T. cruzi* (A chain) and *L. major* (A

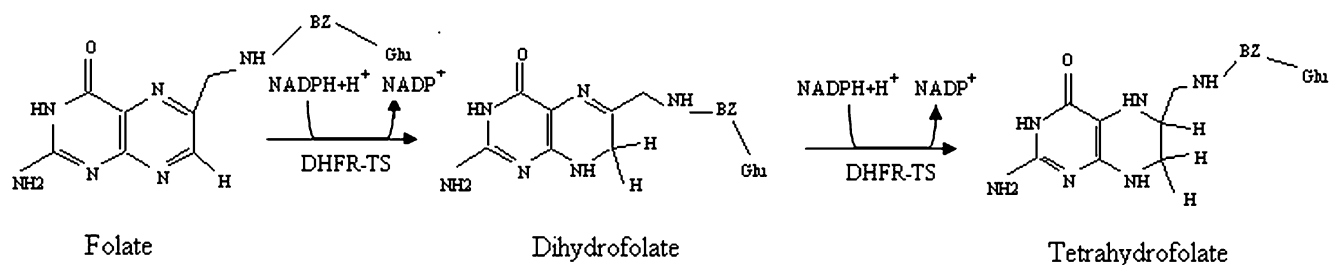


**Fig. 1** Reaction catalyzed by dihydrofolate reductase-thymidylate synthase (DHFR-TS)

and B chains) were aligned using the homology module of Insight II. During sequence alignment, structurally conserved regions (SCRs) common to the templates and the target protein were identified by automatic multiple sequence alignment based on the Needleman-Wunsch algorithm [24].

### 3D model building

The 3D structure of *L. donovani chagasi* DHFR-TS was built using the protein structure-modeling program and homology module of Insight II. An initial 3D-structure of DHFR-TS of *L. donovani chagasi* was obtained by transferring the backbone coordinates of the DHFR-TS from *L. major* and *T. cruzi* residues to the corresponding residues of *L. donovani chagasi* DHFR-TS, except for several variable regions (Loops). The next step in the generation of the 3D model was building the structurally

variable regions (SVRs). A total of ten models were built by using the option ‘Optimize level high’ for the structure. At this point a reasonable model was constructed with a few trivial abnormalities that were further corrected by minimization using the Discover 3 module of Insight II. The model was subjected to minimization in two stages: 100 iterations of steepest descent, followed by 500 iterations of conjugate gradient, to a gradient of 0.001 kcal mol<sup>-1</sup>Å<sup>-1</sup>. Further refinement was done using MD stimulations.

### Validation of the model

A protein 3D model derived from homology modeling techniques may be prone to many sources of inaccuracy; therefore, it is important to assess overall structure quality and to identify regions that may require careful investiga-

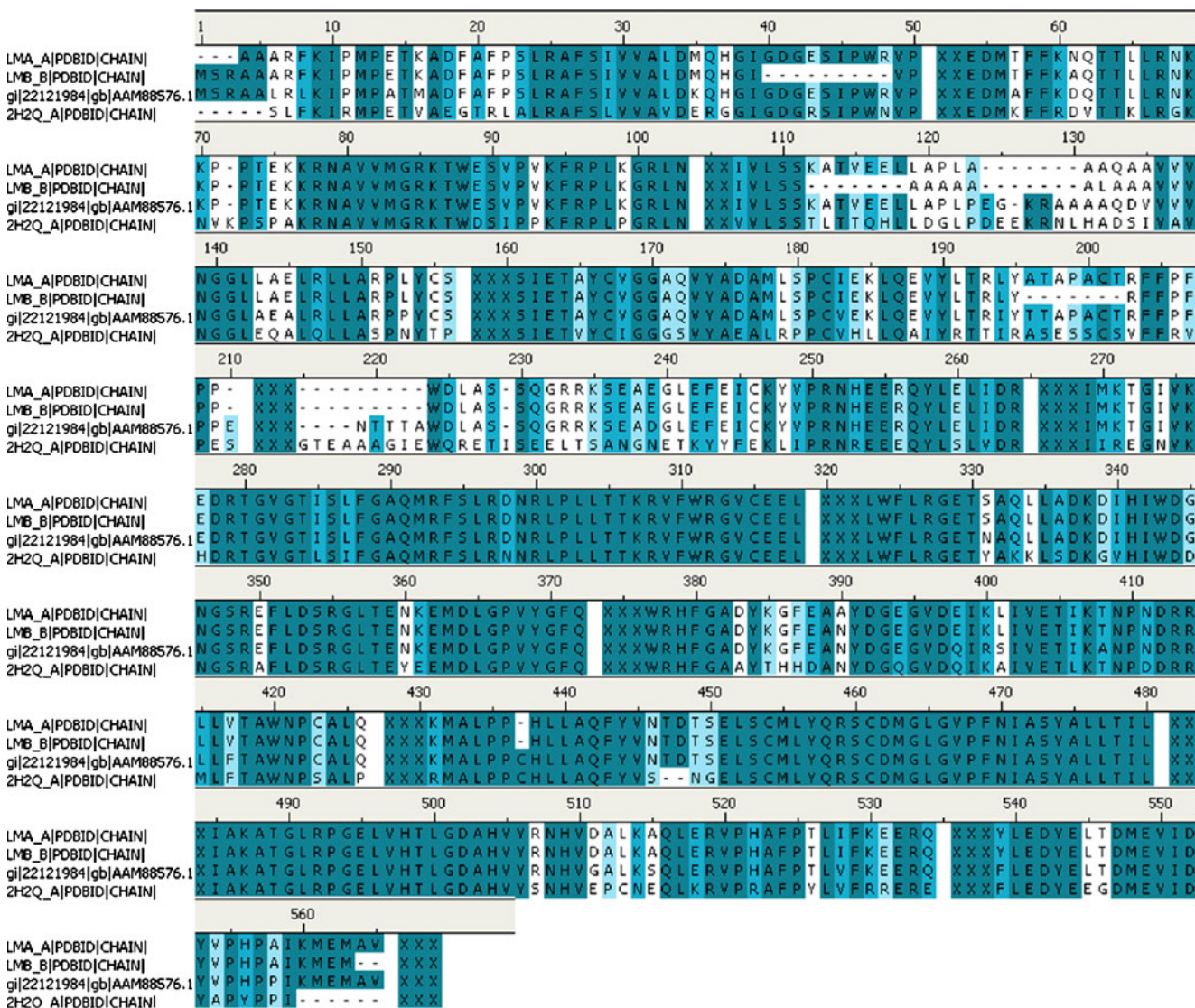


Fig. 2 Multiple sequence alignment of *Leishmania donovani chagasi* DHFR-TS with *L. major* A and B chains and *Trypanosoma cruzi* A chain



tion. Validation of a 3D model is an essential step that can be performed at different levels of structural organization to check the stereochemical parameters and accuracy of the overall folds.

The structure of the refined model was evaluated using the programs PSQS, VERIFY\_3D, ERRAT [25–28], PROSA [29] and PROCHECK [30]. Verify3D analyzes the compatibility of an atomic model (3D) with its own amino acid sequence (1D). Each residue is assigned a structural class based on its location and environment. PROSA uses knowledge-based potentials of mean force to evaluate model accuracy, and shows local model quality by plotting energies as a function of amino acid sequence position. PROCHECK measures the stereochemical quality of the 3D structure. ERRAT is used for geometric environment profile calculation whereas PSQS calculates the local environment profile. The secondary structure of the modeled protein was analyzed using Swiss Protein Databank Viewer (SPDBV) software [31].

#### Preparation of ligand and protein structures for docking

Correct representation of the ligand is necessary for docking studies. The ligand was modeled using the Build/3D-sketcher module of Cerius2 v4.9 [32]. Gastegier charges were added to the modeled structure. In order to obtain lowest energy conformation, the conformation space was first scanned using energy optimization cycles followed by dynamic simulation using the annealing dynamics with user defined attributes: Reqttemp, 500K; dynamic time step, 0.001Ps; Steps, 2000 using constant NVE (constant number of atoms, volume and energy). This was followed by an energy minimization procedure. The force field used was Dreiding and the molecule was minimized to high convergence using 5,000 (or more if required) iterations on the steepest descent followed by conjugate gradient; seven–

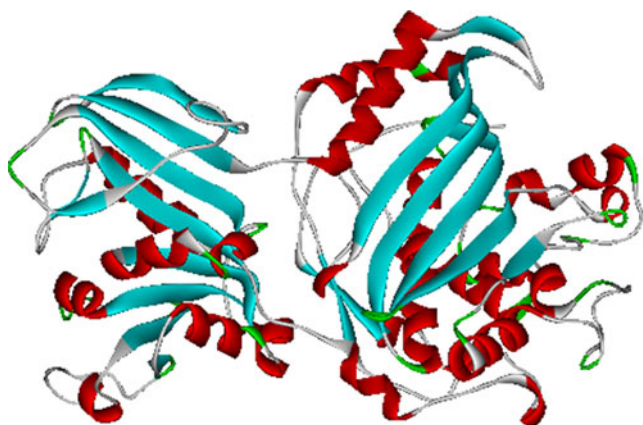


**Fig. 3** Final three-dimensional (3D) structure of *L. donovani chagasi* DHFR-TS. Red  $\alpha$ -helix, cyan  $\beta$ -sheet, green  $\beta$ -turns

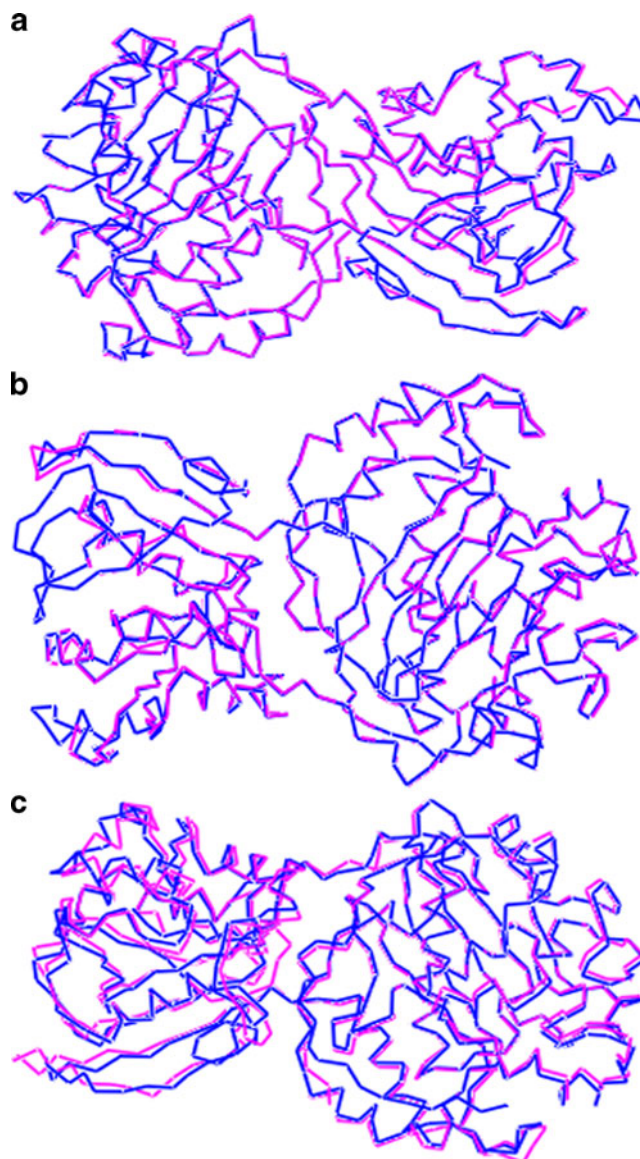


**Fig. 4a–c** Comparison of the 3D model of *L. donovani chagasi* DHFR-TS (blue) with the three templates used (pink). **a** *L. major* A chain, **b** *L. major* B chain, **c** *T. cruzi* A chain

eight runs were performed. The lowest energy structure thus obtained was taken as the final structure. Protonation states were generated corresponding to an aqueous environment at pH 7.4, i.e., hydrogens were added where appropriate.

Protein preparation was carried out using the biopolymer module in Insight II. The protein coordinates were converted to PDB format and proper assignment of residue names and atom types were carried out. The assignment of protonation states is essential because the characterizations of H-bond donor/ acceptors are bound to change if appropriate protonation states are not assigned correctly. Hence, protonation states of the charged residues were assigned by adding the hydrogen atoms at pH 7.4.

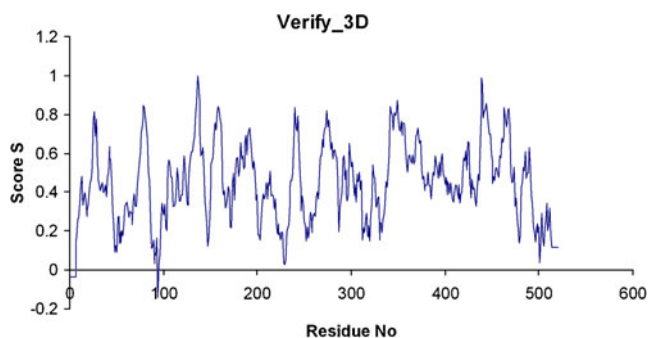


**Fig. 5** Verify-3D results for the *L. donovani chagasi* DHFR-TS model; residues with positive compatibility score are reasonably folded

### Docking studies

A docking study was performed to explore the docking modes of the ligand into the protein binding site. MTX is a well known substrate that binds the DHFR-TS protein. The 3D structure of MTX was docked into the active site of *L. donovani chagasi* DHFR-TS. GOLD is a well-known automated ligand-docking program that uses a genetic algorithm (GA) to explore the full range of ligand conformational flexibility with partial flexibility of the protein side chains.

The default calculation mode, which provides the most accurate docking results, was selected for all calculations. In the standard calculation mode, by default, the GA run comprised of 100,000 genetic operations on an initial

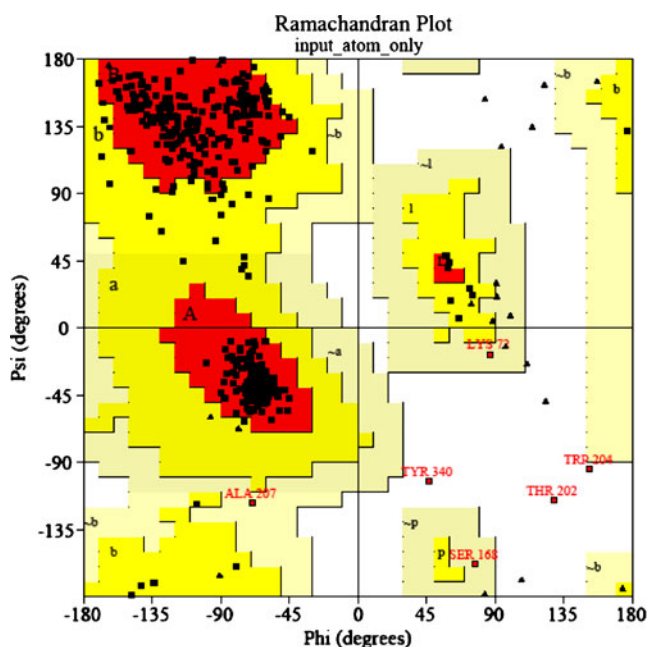


**Fig. 6** Ramachandran plot of *Leishmania donovani chagasi* DHFR-TS obtained using PROCHECK

**Table 1** The  $\Phi$ ,  $\phi$  region percentages as calculated by PROCHECK

Position of residue	No. of amino acids	% in region
Most favored regions	410	90.5
Additional allowed regions	37	8.2
Generously allowed regions	3	0.7
Disallowed regions	3	0.7

population of 100 members divided into five subpopulations, and the annealing parameters of fitness function were set at 4.0 for van der Waals and 2.5 for hydrogen bonding interactions. Default values were selected for other parameters as well. The number of generated poses was set to 20 and top ranked solutions (15) were retained. Chemscore scoring function was used to identify docking poses as well as to rank these poses.

### Results and discussion

#### Homology modeling of *L. donovani chagasi* DHFR-TS

In this study, we focused on generating a 3D model for *L. donovani chagasi* DHFR-TS suitable for docking studies. A high degree of sequence matching is essential for the success of homology modeling. Two reference proteins—*L. major* DHFR-TS (A and B chains) and *T. cruzi* DHFR-TS (A chain)—were used to model the structure of *L. donovani chagasi* DHFR-TS. The *T. cruzi* DHFR-TS sequence was used as a template to compensate for gaps present in *L. major* DHFR-TS (A and B chains), and also for regions in the target protein that did not match those of *L. major*, so that a more accurate 3D structure could be modeled. The homology scores for the target with the two reference proteins *L. major* DHFR-TS (A and B chains) and *T. cruzi* DHFR-TS (A chain) were 90 % and 66%, respectively. The DHFR-TS enzymes from different organisms exhibit extensive sequence similarity and share a common mechanism. The sequence alignment results suggest that there is a high degree of conservation between *L. donovani chagasi* DHFR-TS and *L. major* DHFR-TS. The final alignment of

**Table 2** PROCHECK results for modeled *L. donovani chagasi* dihydrofolate reductase-thymidylate synthase (DHFR-TS) protein

Type of residue	No. of amino acids
Non glycine and non proline	453
End residues (excl Gly and pro)	2
Glycine	33
Proline	32

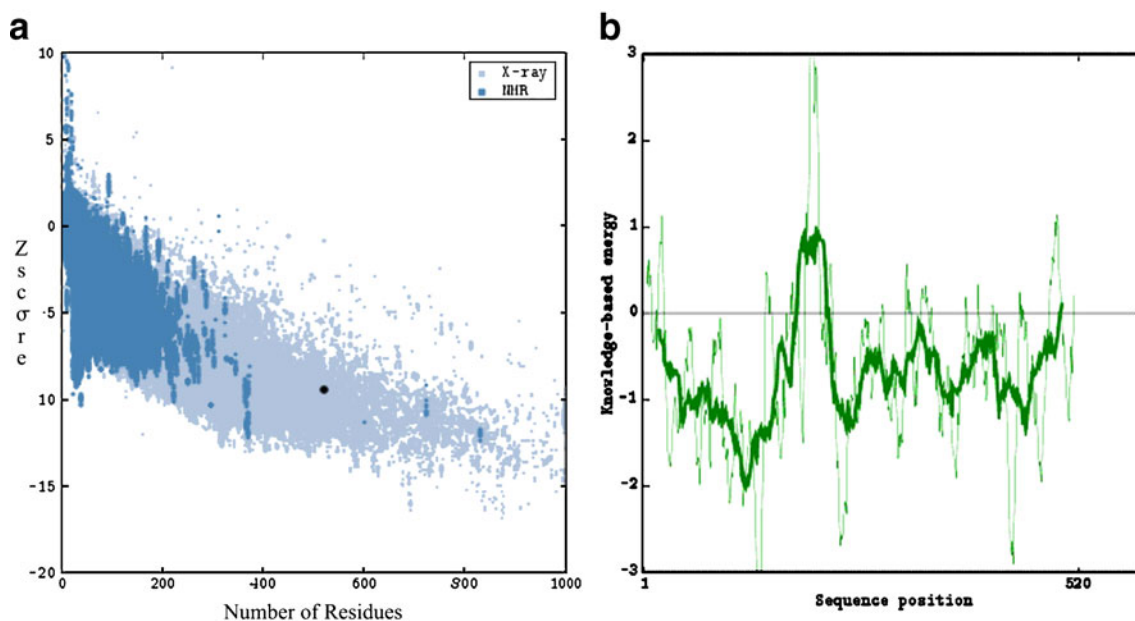


**Fig. 7** **a** ProSA-web Z-scores of all protein chains in the protein databank (PDB) determined by X-ray crystallography (light blue) and NMR spectroscopy (dark blue) with respect to their length. The Z-

score of *L. donovani chagasi* DHFR-TS was present within the range represented by the black dot. **b** Energy profile drawn for *L. donovani chagasi* DHFR-TS using the PROSA program

the target sequence with the deduced amino acid sequences of DHFR-TS from *L. major* X-ray crystal structure (kindly supplied by D. Matthews, Agouron Pharmaceuticals) and *T. cruzi* (PDB Id: 2H2Q) is shown in Fig. 2. A total of 63.6% SCRs were identified, accounting for most of the total sequence. The remaining parts of the sequence, i.e., SVRs, were not in close proximity to the binding pocket. The loop searching algorithm was used to construct the structure of loops between SCRs and, with this procedure, initial modeling was completed. The modeled structure was further refined by energy minimization, followed by MD simulations. The modeled 3D structure of *L. donovani chagasi* DHFR-TS (Fig. 3) shows that it has 15 stranded  $\alpha$ -helices with 22-stranded  $\beta$ -sheets. Superimposition of the generated model with *L. major* (A and B chains) and *T. cruzi* (A chain) is shown in Fig. 4. Root mean square deviation (RMSD) values of 0.69 Å with *L. major* (A chain), 0.71 Å with *L. major* (B chain) and 1.11 Å with *T. cruzi* (A chain) indicated a good overall structure alignment with the templates.

#### Validation of modeled structure

The final structure with lowest energy was checked by Verify-3D (Fig. 5); the self-compatibility score for this protein is 204.26, which is much higher than the lowest score (66.02) and close to the top score (237.66). Some of the residues present in the binding site, e.g., Lys90, Arg92, Lys95 and Gly96, have low self-compatibility scores; however, the values are within the acceptable range. This

indicates that these residues are in the correct folded state and are not misfolded [26]. Only Leu94, which is not important for inhibition of DHFR-TS, has a self-compatibility score below the acceptable range. These low scores may be due to the fact that the conserved residues present in this region of the templates also have low self-compatibility scores. The structure of *L. donovani chagasi* DHFR-TS was further validated by the programs PROCHECK and PROSA. The reliability of the backbone torsion angles  $\Phi$ ,  $\phi$  of the modeled protein was examined by PROCHECK, and the Ramachandran plot is shown in Fig. 6. The values of core, allowed, generously allowed and disallowed regions, and type of residues for the *L. donovani*

**Table 3** Scores of *L. donovani chagasi* DHFR-TS and template structures using different programs. *T* Template

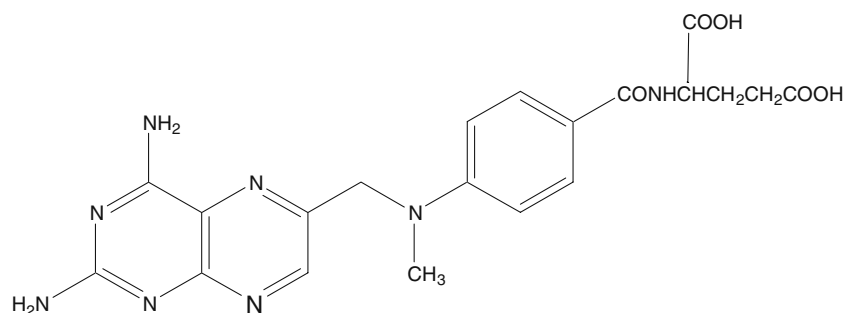
Structure	ERRAT <sup>a</sup>	PSQS <sup>b</sup>	PROSA Z-Score <sup>c</sup>
<i>L. donovani chagasi</i> DHFR-TS	76.712	-0.2157	-9.78
<i>L. major</i> A DHFR-TS ( <i>T</i> )	87.40	-0.2064	-7.99
<i>L. major</i> B DHFR-TS ( <i>T</i> )	88.20	-0.2056	-6.88
<i>Trypanosoma cruzi</i> A DHFR-TS ( <i>T</i> )	93.186	-0.2628	-10.74

<sup>a</sup> Percentage of the protein for which the calculated error value falls below the 95% rejection limit

<sup>b</sup> The average value for the PSQS scores of a representative set of PDB structures is -0.27, and most structures have a PSQS less than -0.1

<sup>c</sup> Z-score of the input structure is within the range of scores typically found for native proteins of similar size



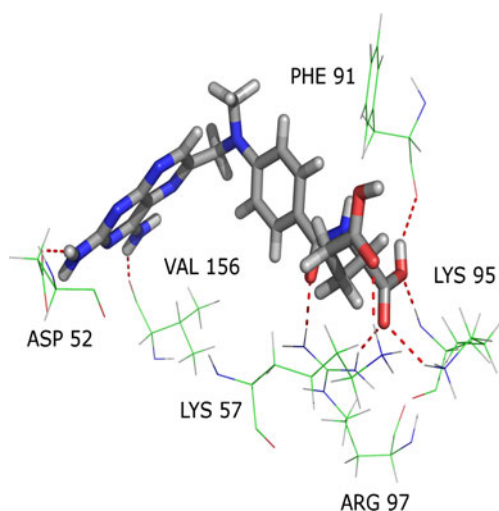
**Fig. 8** Structure of the DHFR inhibitor methotrexate (MTX)

*chagasi* DHFR-TS model are shown in Tables 1 and 2, respectively. Only three residues—Tyr340, Thr202 and Trp204—are in disallowed region. Validation of the modeled structure with ProSA-web reveals that the Z-score value of  $-9.78$  (Fig. 7a) is within the range of native conformations of the crystal structures (Table 3). ProSA-web analysis shows the overall residue energies of the *L. donovani chagasi* DHFR-TS model (Fig. 7b). The plot shows local model quality by plotting energies as a function of amino acid sequence position. The plot is smoothed by calculating the average energy over each residue fragment, which is then assigned to the central residue of the fragment (Fig. 7b, thick line). A second line with a smaller window size of ten residues is shown in the background of the plot (Fig. 7b, thin line). A further quality check of the modeled structure was carried out using programs such as ERRAT and PSQS, and their quality scores are shown in Table 3.

#### Docking studies

To understand the interaction between the *L. donovani chagasi* DHFR-TS binding site and MTX (Fig. 8), docking

studies were carried out using Gold Docking program. The predicted binding mode of MTX in the binding site of the protein shows crucial hydrogen bonding interactions with the binding site residues Arg97, Phe91, Lys95, Lys57, Val156 and Asp52 (Fig. 9). In our model, the amino groups present in the 2- and 4- positions of the pteridine moiety of MTX form hydrogen bonds with the carboxylic group of Asp52 and with the backbone carbonyl oxygen of Val156. The carbonyl oxygen attached to the phenyl ring of MTX forms a hydrogen bond with one of the side chain amino groups of Arg97. The hydrogen of the alpha carboxyl group present in MTX forms a hydrogen bond with the backbone carbonyl oxygen of Phe91. The hydroxyl oxygen of the alpha carboxyl group forms a hydrogen bond with the backbone amino group of Lys95, while the carbonyl oxygen forms a bifurcated hydrogen bond with the side chain amino groups of Arg97 and Lys95. The carbonyl oxygen of the gamma carboxyl group of MTX forms a hydrogen bond with the side chain amino group of Lys57. Hydrophobic interactions and their distances observed using LIGPLOT [33] are listed in Table 4. These interactions corroborate very well with the interactions found in the MTX-bound *L. major* crystal structure.

**Fig. 9** Hydrogen bonding interactions of the binding site residues of *L. donovani chagasi* DHFR-TS with MTX (in pymol)**Table 4** Hydrophobic interactions of *L. donovani chagasi* DHFR-TS with methotrexate (MTX) in LIGPLOT

Atom 1	Atom type	Atom 2	Atom type	Distance (Å)
MTX	C26	Lys 95	CG	3.47
MTX	C17	Phe 91	CD2	3.89
MTX	C17	Phe 91	CB	3.52
MTX	C15	Pro 88	CD	3.52
MTX	C18	Val 87	CG1	3.41
MTX	C17	Val 87	CG1	3.71
MTX	C15	Val 87	CA	3.75
MTX	C29	Lys 57	CD	3.29
MTX	C13	Met 53	CE	3.89
MTX	C13	Met 53	SD	3.53

## Conclusions

In the absence of a crystallographic structure of *L. donovani chagasi* DHFR-TS, we present in this paper a homology model of *L. donovani chagasi* DHFR-TS using the currently available X-ray structures of *L. major* and *T. cruzi* DHFR-TS as templates. Careful energy minimization and MD simulation of the model led to a high quality 3D structure of *L. donovani chagasi* DHFR-TS, as judged by PROCHECK, VERIFY\_3D, PROSA, ERRAT and PSQS. The final refined model was superimposed with the templates *L. major* A chain, *L. major* B chain and *T. cruzi* A chain and showed RMS deviations of 0.69 Å, 0.71 Å and 1.11 Å, respectively. A flexible docking study performed using MTX as the ligand in the binding site of the *L. donovani chagasi* DHFR-TS model showed that the generated model has close similarity to *L. major* DHFR-TS. The hydrogen bond and hydrophobic interactions present in the X-ray crystal structure of *L. major* DHFR-TS bound to MTX were also present in the *L. donovani chagasi* DHFR-TS model. Val156, Val30, Lys95, Lys75 and Arg97 are the key amino acid residues within the *L. donovani chagasi* DHFR-TS binding pocket that play an important role in ligand or substrate binding. This observation clearly shows that the generated model is comparable to the X-ray crystal structure of *L. major*, and that the binding mode of MTX is very similar in both *L. donovani chagasi* and *L. major*. The high level of structural similarity between the *L. donovani chagasi* and *L. major* DHFR-TS enzymes suggests that compounds that inhibit one enzyme selectively will possibly inhibit the other. This information will be very useful in the future design of potential drugs against leishmaniasis.

**Acknowledgments** The authors thank the Council for Scientific and Industrial Research (CSIR), New Delhi, India, for providing financial assistance from a grant under Mission Mode Program CMM 0017. We thank Prof. David A. Matthews, Agouron Pharmaceuticals, San Diego, CA, for providing the coordinates of the *Leishmania major* crystallographic structure. L.M. and P.M. thank CSIR, New Delhi, India, for Project Assistantship.

## References

- Cunha AM, Chagas E (1937) New species of protozoa of the genus *Leishmania* pathogenic to man *Leishmania chagasi* n. sp previous note. O Hospital 11:3–9
- Croft SL, Coombs GH (2003) Leishmaniasis—current chemotherapy and recent advances in the search for novel drugs. Trends Parasitol 19:502–508. doi:10.1016/j.pt.2003.09.008
- Guerin PJ, Olliaro P, Sundar S, Boelaert M, Croft SL, Desjeux P, Wasunna MK, Bryceson ADM (2002) Visceral leishmaniasis: current status of control, diagnosis, and treatment, and a proposed research and development agenda. Lancet Infect Dis 2:494–501. doi:10.1016/S1473-3099(02)00347-X
- Davies CR, Kaye P, Croft SL, Sunder S (2003) Leishmaniasis: new approaches to disease control. BMJ 326:377–382. doi:10.1136/bmj.326.7385.377
- Desjeux P (2001) Worldwide increasing risk factors for leishmaniasis. Med Microbiol Immunol 190:77–79. doi:10.1007/s004300100085
- World Health Organization (2000) The Leishmaniasis and Leishmania/HIV co-infections. Fact Sheet Number 116. WHO, Geneva, Switzerland
- Shafinaz FC, Villamor VB, Guerrero RH, Leal I, Brun R, Croft SL, Goodman JM, Maes L, Ruiz-Perez LM, Pacanowska DG, Gilbert IH (1999) Design, synthesis, and evaluation of inhibitors of trypanosomal and leishmanial dihydrofolate reductase. J Med Chem 42:4300–4312. doi:10.1021/jm981130+
- Decampo R (2001) Recent developments in the chemotherapy of Cha-gas' disease. Curr Pharm Des 7:1157–1164. doi:10.2174/1381612013397546
- McLuskey K, Gibellini F, Carvalho P, Avery MA, Huntera WN (2004) Inhibition of *Leishmania major* pteridine reductase by 2, 4, 6-triaminoquinazoline: structure of the NADPH ternary complex. Acta Cryst 60:1780–1785. doi:10.1107/S0907444904018955
- Ferone R, Roland S (1980) Dihydrofolate reductase: thymidylate synthase, a bifunctional polypeptide from *Crithidia fasciculata*. Proc Natl Acad Sci USA 77:5802–5806
- Garrett CE, Coderre JA, Meek TD, Garvey EP, Claman DM, Beverly SM, Santhi DV (1984) A Bifunctional thymidylate synthase-dihydrofolate reductase in protozoa. Mol Biochem Parasitol 11:257–265. doi:10.1016/0166-6851(84)90070-7
- Ivanetich KM, Santhi DV (1990) Bifunctional thymidylate synthase-dihydrofolate reductase in protozoa. FASEB J 4:1591–1597. doi:0892-6638/90/0004-1591/\$01.50
- Birmingham A, Derrick JP (2002) The folic acid biosynthesis pathway in bacteria: evaluation of potential for antibacterial drug discovery. BioEssays 24:637–648. doi:10.1002/bies.10114
- Walsh C (2003) Antibiotics: actions, origins, resistance. ASM, Washington. doi:10.1110/ps.041032204
- Then RL (2004) Antimicrobial dihydrofolate reductase inhibitors—achievements and future options: review. J Chemother 16:3–12
- Zheng QC, Li ZS, Sun M, Zhang Y, Sun CC (2005) Homology modeling and substrate binding study of nudix hydrolase Ndx1 from *Thermos thermophilus* HB8. Biochem Biophys Res Commun 333:881–887
- Xu W, Cai P, Yan M, Xu L, Ouyang PK (2007) Molecular docking of xylitol and xylose isomerase from *Thermus thermophilus* and model analysis. Chem J Chin Univ 28:971–973
- He YP, Hu HR, Xu LS (2005) Structure–activity relationship studies on 6-naphthylmethyl substituted HEPT derivatives as nonnucleoside reverse transcriptase inhibitors based on molecular docking. Chem J Chin Univ 26:254–258
- Knighton DR, Kan CC, Howland E, Janson CA, Hostomska Z, Welsh KM, Matthews DA (1994) Structure of and kinetic channelling in bifunctional dihydrofolate reductase-thymidylate synthase. Nat Struct Biol 1:186–194. doi:10.1038/nsb0394-186
- Senkovich O, Schormann N, Chattopadhyay D (2009) Structures of dihydrofolate reductase-thymidylate synthase of *Trypanosoma cruzi* in the folate-free state and in complex with two antifolate drugs, trimetrexate and methotrexate. Acta Cryst 65:704–716. doi:10.1107/S090744490901230X
- InsightII (2007) Accelrys, San Diego
- GOLD (2006) CCDC, Cambridge
- http://www.pymol.org
- Needleman SB, Wunsch CD (1970) A general method applicable to the search for similarities in the amino acid sequence of two proteins. J Mol Biol 48:443–453. doi:10.1016/0022-2836(70)90057-4
- Jaroszewski L, Pawlowski K, Godzik A (1998) Multiple model approach: exploring the limits of comparative modeling. J Mol Model 4:294–309. doi:10.1007/s008940050087



26. Luthy R, Bowie JU, Eisenberg D (1992) Assessment of protein models with three-dimensional profiles. *Nature* 356:83–85. doi:[10.1038/356083a0](https://doi.org/10.1038/356083a0)
27. Colovos C, Yeates TO (1993) Verification of protein structures: patterns of nonbonded atomic interactions. *Protein Sci* 2:1511–1519. doi:[10.1002/pro.5560020916](https://doi.org/10.1002/pro.5560020916)
28. Hoof RWW, Vriend G, Sander C, Abola EE (1996) Errors in protein structures. *Nature* 381:272–272. doi:[10.1038/381272a0](https://doi.org/10.1038/381272a0)
29. Sippl MJ (1993) Boltzmann's principle, knowledge-based mean fields and protein folding. *J Comput Aided Mol Des* 7:473–501. doi:[10.1007/BF02337562](https://doi.org/10.1007/BF02337562)
30. Laskowski RA, Macarthur MW, Moss DS, Thornton JM (1993) PROCHECK a program to check the stereo chemical quality of protein structure. *J Appl Cryst* 26:283–291. doi:[10.1107/S0021889892009944](https://doi.org/10.1107/S0021889892009944)
31. Guex N, Peitsch MC (1997) SWISS MODEL and the Swiss pdb viewer: an environment for comparative protein modeling. *Electrophoresis* 18:2714–2723. doi:[10.1093/nar/gkg520](https://doi.org/10.1093/nar/gkg520)
32. Cerius2 (2006) Accelrys, San Diego
33. Wallace AC, Laskowski RA, Thornton JM (1995) LIGPLOT: a program to generate schematic diagrams of protein–ligand interactions. *Protein Eng* 8:127–134. doi:[10.1093/protein/8.2.127](https://doi.org/10.1093/protein/8.2.127)